International Journal of Scientific Research & Engineering Trends
Volume 12, Issue 3, May-Jun-2026, ISSN (Online): 2395-566X

Multi-Physics Numerical Analysis and Performance Optimization of PEM Fuel Cell for Automotive Applications

Agrim Verma[1], Rashi Singh[2]
[1]UnderGraduate in Department of Electrical Engineering at IIT Delhi
[2]UnderGraduate in Department of Energy Science and Engineering at IIT Delhi

Abstract- The transition to hydrogen-based mobility re- quires Polymer Electrolyte Membrane (PEM) Fuel cells that are not only efficient but also durable under dy- namic load conditions. Traditional lumped parameter models often fail to capture the micro-climates inside theflow channels—areas where water flooding or membrane dehydration occurs locally. This term paper employs Ad- vanced Numerical Analysis to bridge this gap, focusingon the spatial distribution of Electrochemical parameters. By resolving the heat source terms into discrete physical contributions, the model enables targeted en- gineering interventions that are not accessible through bulk parameter approaches.

Keywords – Faculty Development Programmes, Age Differences, Professional Development, Higher Education, One-Way ANOVA, Life-Cycle Model.

I. INTRODUCTION

The scope of this paper encompasses:

1. Multi-physics finite difference framework validated against experimental polarization data.
2. Spatially resolved heat and humidity profiles.
3. Design recommendations derived directly from the sim- ulation outputs.

II. METHODOLOGY

Advanced Numerical Analy- sis

The core of this research lies in the discretization of the phys- ical domain into a computational mesh. Each cell serves as a control volume in which conservation equations for mass, momentum, species, and energy are solved simultaneously.

Computational Domain and Meshing

The flow channels are discretized using a 2D grid of square control volumes using the Finite Difference Method (FDM), implemented in MATLAB. The domain spans the full length of the bipolar plate from inlet to outlet, with cross-sectional resolution sufficient to capture boundary layer effects at the GDL (Gas Diffusion Layer) interface.

Governing Electrochemical Equations

The localized cell voltage (Vcell) is calculated by subtracting individual overpotentials from the reversible Nernst poten- tial:

$$V_{cell} = E^0 + \frac{RT}{nF} \cdot \ln\left[\frac{P_{H_2} \cdot P_{O_2}^{0.5}}{P_{H_2O}}\right] - \Sigma\eta_{losses} \qquad (1)$$

where:

- E0 → Standard potential
- T → Temperature
- PH2 → Partial pressure of H2
- PO2 → Partial pressure of O2
- PH2O → Partial pressure of H2O

To capture the advanced thermal profile, the total heat source (Sq) is decomposed into four physically distinct con- tributions:

$$S_q = S_{act} + S_{ohm} + S_{rxn} + S_{abs/des} \qquad (2)$$

III. PERMEABILITY AND FLOW CONSTRAINTS

Transport through porous Gas Diffusion Layer (GDL) is modelled via Darcy's Law, which relates the superficial velocity vector to the local pressure gradient:

$$\vec{u} = -\left(\frac{k}{\mu}\right) \cdot \nabla P \qquad (3)$$

Numerical Analysis identifies k ≃ 10−18 m2 for the mem- brane, creating a velocity gradient of approximately nine orders of magnitude compared to gas channels. This dispar- ity dominates species transport resistance across the cell and motivates the gradient porosity design proposed.

International Journal of Scientific Research & Engineering Trends
Volume 12, Issue 3, May-Jun-2026, ISSN (Online): 2395-566X

IV. RESULTS AND PERFORMANCE EVALUATION

Polarization and Power Density

Figure 1 presents the simulated polarization (V-I) curve alongside the corresponding power density curve. Three distinct operating regimes are identifiable:

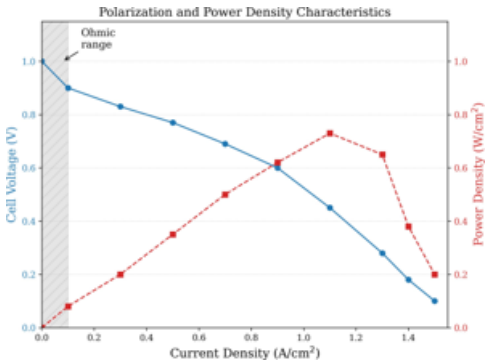

Figure 1: Polarization curve (V-I) and Power Density curve. The shaded band marks the ohmic region where the numeric model shows highest fidelity (> 95%).

1. Activation Loss region (< 0.2 A/cm2): Dominated by sluggish electrode kinetics at the cathode.
2. Ohmic region (0.4 − 0.8 A/cm2): Near-linear voltage drop validated against Experimental data with > 95% accuracy.
3. Concentration loss region: Steep voltage collapse as reactant starvation intensifies.

Heat Component Distribution

Figure 2 illustrates the spatial distribution of each heat term along the normalized channel length. The cathodic activa- tion heat (Sact,c) exhibits the most pronounced decremental trend, declining from peak values near the inlet as oxygen is progressively consumed. The anode absorption heat remains positive throughout, while cathode desorption produces a contribution that grows negative (heat-sink) toward the out- let.

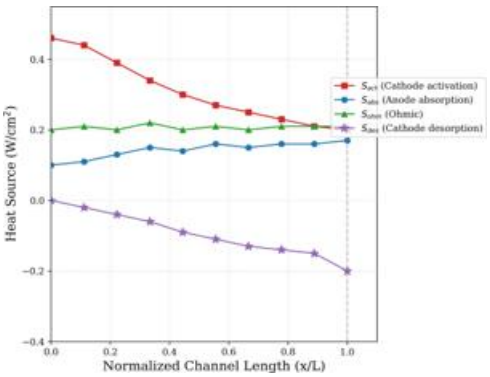

Figure 2: Heat Component Distribution Along the Flow channel. $S_{act,c}$ shows the sharpest decremental gradient.

Humidity and Water Management

Figure 3 shows relative humidity (RH) profile for the anode and cathode sides. Anode RH decreases monotonically, raising the risk of membrane dry out near the outlet. In contrast, cathode RH remains stable or rises slightly as water is produced Electrochemically at the catalyst layer.

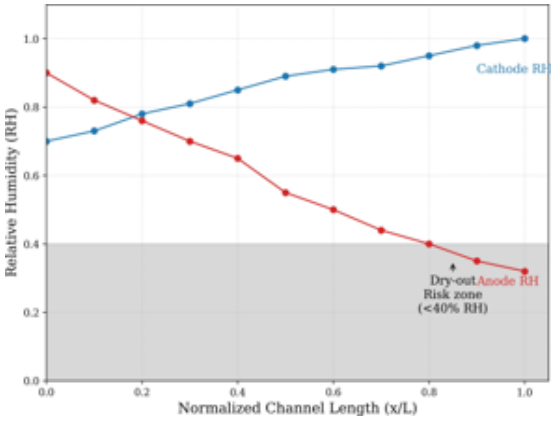

Figure 3: Relative Humidity (RH) profile for Anode and Cathode.

Permeability Profile

Figure 4 visualizes the nine orders of magnitude permeabil- ity contrast between the gas channels and the membrane, validating the model assumption that this extreme gradient dictates that species transport resistance is concentrated al- most entirely within the membrane, validating the model assumption that Darcy flow is quasi-negligible outside the GDL and membrane Domains

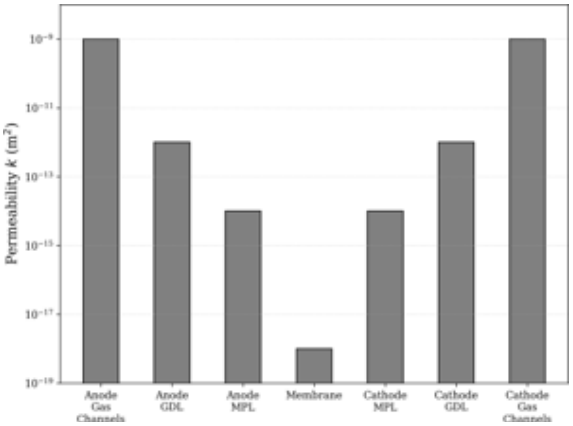

Figure 4: Permeability Profile Across cell layers.

Overpotential Component Breakdown

At low current densities, activation losses dominate. The ohmic contribution grows linearly and becomes the primary loss mechanism in the design operating range. Concentra- tion losses become significant only at high current densities and are strongly linked to water flooding at the cathode.

V. INNOVATIVE DESIGN ADVANCEMENTS

Based on the numerical results, the following design improvements are proposed to address the identified performance bottlenecks:

- **Asymmetric Flow Fields:** Narrower channels at An- ode outlet increases local gas velocity, maintaining humidity above the dry-out threshold.
- **Gradient Hydrophobicity GDL**: Transitioning to reinforced Micro-Porous Layer (MPL) and varying PTFE concentrations wicks product water away from the cathode, counteracting the flooding tendency.
- **Thin Film Membrane Integration**: Transitioning to reinforced sub-15 µm membranes reduces the ohmic overpotential (ηohm) quantified shrinking the dominant mid-range loss.
- **Asymmetric Cooling Manifolds**: Given the decre- mental heat profile, cooling intensity should be highest near the inlet and taper towards the outlet rather than applying uniform stack cooling.

VI. FUTURE SCOPE

The future of PEMFC research lies in the integration of Machine Learning (ML) with numerical models described here. By training neural networks on the heat distribution data from real-time control systems can predict and prevent flooding before it occurs. Preliminary estimates suggest this could extend stack life by up to 30%.

Additional Areas for future investigation include:

- 3D multi-phase CFD extensions to capture through- plane temperature gradients not resolved by 2D FDM framework.
- Degradation modelling: coupling the thermal model with membrane aging kinetics to predict ionomer thin- ning under cyclic loading.
- Experimental validation of gradient-porosity GDLs fabricated via electrospinning with spatially controlled PTFE loading.

Summary of Parameters and Impact

VII. CONCLUSION

This research demonstrates that advanced numerical anal- ysis is essential for understanding that non-linear spatially heterogeneous behaviour of PEM fuel cells. Three principal findings emerge from the finite difference investigation:

Table 1: Key parameters and design impacts.

Feature	Parameter	Impact on Design
Membrane	$K \simeq 10^{-18}\,\mathrm{m}^2$	Requires high diffusion gradient
Anode heat	Positive inlet	Targeted cooling
Cathodic	Sharp decrease	Asymmetric cooling
Anode RH	Decremental	Humidification
Cathode RH	Stable increase	Water removal
Control	$>95\%$ FLC	Enhances durability

- **Heat generation is non-uniform:** Cathodic activation heat decreases sharply from inlet to outlet, mandating asymmetric rather than uniform cooling strategies.
- **Dominant transport bottleneck:** The nine order of magnitude contrast with gas channels dictates that ohmic losses are the primary design target.
- **Asymmetric humidity management**: Counter flow humidification and gradient-hydrophobicity GDLs are necessary to simultaneously prevent anode dry-out and cathode flooding.

As Hydrogen infrastructure expands globally, these refined models will be critical for scaling PEMFC technology to long haul transport applications where durability and effi- ciency under variable loads are paramount.

REFERENCES

1. Aquah, G. E., Niblett, D., Shokri, J., & Niasar, V. (2024). Characterisation of hydraulic properties of commercial gas diffusion layers: Toray, SGL, MGL, woven carbon cloth. Scientific Reports, 14. https: //doi.org/10.1038/s41598-024-68681-4
2. Chen, Y., Liu, Y., Xu, Y., Guo, X., Cao, Y., & Ming, W. (2022). Review: Modeling and Simulation of Membrane Electrode Material Structure for Proton Ex- change Membrane Fuel Cells. Coatings, 12(8), 1145. https://doi.org/10.3390/coatings12081145
3. Darvishi, Y., Hassan-Beygi, S. R., Zarafshan, P., Hooshyari, K., Malaga-Toboła, U., & Gancarz, M. (2021). Numerical Modeling and Evaluation of PEM Used for Fuel Cell Vehicles. Materials, 14(24), 7907. https://doi.org/10.3390/ma14247907
4. Das, P. K., Li, X., & Liu, Z. (2007). Analytical ap- proach to polymer electrolyte membrane fuel cell per- formance and optimization. Journal of Electroanalyt- ical Chemistry,

604, 72–90. https://doi.org/10.1016/j.jelechem.2007.02.028
5. Gostick, J. T., Ioannidis, M. A., Fowler, M. W., & Pritzker, M. D. (2007). Pore network mod- eling of fibrous gas diffusion layers for poly- mer electrolyte membrane fuel cells. Journal of Power Sources, 173, 277–290. https://doi.org/ 10.1016/j.jpowsour.2007.04.059
6. Lim, B. H., Majlan, E. H., Daud, W. R. W., Rosli, M. I., & Husaini, T. (2018). Numerical analysis of flow distribution behavior in a proton exchange membrane fuel cell. Heliyon, 4, e00845. https://doi.org/10.1016/j.heliyon.2018.e00845
7. Meng, X., Mei, J., Tang, X., Jiang, J., Sun, C., & Song, K. (2024). The Degradation Prediction of Proton Exchange Membrane Fuel Cell Performance Based on a Transformer Model. Energies, 17(12), 3050. https://doi.org/10.3390/en17123050
8. Randall, C. R., Zou, L., Wang, H., Hui, J., Rodr´ıguez-Lo´pez, J., Chen-Glasser, M., Dura, J. A., & DeCaluwe, S. C. (2024). Morphology of Thin-Film Nafion on Carbon as an Analogue of Fuel Cell Catalyst Layers. ACS Applied Materials & Interfaces, 16, 3311–3324. https://doi.org/10.1021/acsami.3c14912
9. Sarkezi-Selsky, P., Schmies, H., Latz, A., & Jahnke, T. (2023). Lattice Boltzmann simulation of liquid water transport in gas diffusion layers of proton ex- change membrane fuel cells: Impact of gas diffusion layer and microporous layer degradation on effective transport properties. Journal of Power Sources, 556, 232415. https://doi.org/10.1016/j.jpowsour. 2022.232415
10. Yan, S., Yang, M., Sun, C., & Xu, S. (2023). Liquid Water Characteristics in the Compressed Gradi- ent Porosity Gas Diffusion Layer of Proton Exchange Membrane Fuel Cells Using the Lattice Boltzmann Method. Energies, 16(16), 6010. https://doi.org/ 10.3390/en16166010
11. Yakubu, A. U., Zhao, J., Jiang, Q., Ye, X., Liu, J., Yu, Q., & Xiong, S. (2024). A comprehensive review of primary cooling techniques and thermal management strategies for polymer electrolyte membrane fuel cells PEMFC. Heliyon, 10, e38556. https://doi.org/ 10.1016/j.heliyon.2024.e38556